Al-Azhar Engineering 16th International Conference

Vol. 19, No. 72, July 2024, 20 - 36

THERMAL PERFORMANCE INVESTIGATION OF PLATE-FINNED VAPOR CHAMBER HEAT SINK WITH USING DIFFERENT FLUIDS

Mohammed A. Al-Rahman[1,*], Saeed A.A. Ibrahim[2] , Sayed Ahmed[2], M. Elfaisal Elrefaie1[1]

[1]Mechanical Engineering Department, Faculty of Engineering, Al-Azhar Unversity, Cairo, Egypt.

[2]Mechanical Engineering Department, Faculty of Engineering, Zagazig Unversity, Zagazig, Egypt.

*Correspondence: mohammadabdoel-rahman.18@azhar.edu.eg

Citation:

M.A. Al-Rahman, S.A.A. Ibrahim, S. Ahmed and M.E. Elrefaie, "Thermal Performance Investigation of Plate-Finned Vapor Chamber Heat Sink With Using Different Fluids", Journal of Al-Azhar University Engineering Sector, vol. 19, pp. 20 - 36, 2024.

Received: 29 October 2023

Revised: 01 December 2023

Accepted: 10 December 2023

DoI:10.21608/auej.2023.246427.1460

ABSTRACT

The vapor chamber (VC) is considered one of the most effective approaches for heat dissipation in electronic components. This study investigates experimentally the thermal characteristics of a novel wickless vapor chamber integrated with a plate-finned heat sink (PFHS) to identify the optimal operating conditions of VC and enhance this condition by using different fluids. The study examines the influence of various parameters such as Reynolds number, heat input, filling ratio, operating vacuum pressure, and different fluids (distilled water and propylene glycol solutions) on VC's thermal performance. To prove the effectiveness of the VC, the thermal characteristics of the plate-finned heat sink (PFHS) with and without VC are compared. The results demonstrate that utilizing a VC leads to a significantly more uniform temperature distribution along the base of the PFHS and low overall temperatures. Conversely, in the absence of a VC, the PFHS exhibits a non-uniform temperature distribution, with a bell-shaped profile and concentrated high temperatures at the center at the same operating conditions. Based on the experimental results, over the heat inputs range (10 – 90 W), the lowest thermal resistance and heater temperature occur at 50% filling ratio (FR) with the operating vacuum pressure = 1kPa. The VC's thermal performance improves with using propylene glycol solution at low heat input.

KEYWORDS: Vapor chamber, Thermal performance, Heat sink, Thermal resistance.

دراسة الأداء الحراري للبالوعة الحرارية لغرفة البخار ذات الزعانف المسطحة مع أستخدام سوائل مختلفة

محمد عبدالرحمن[1*]، سعيد عبدالله[2]، سيد أحمد[2]، محمد الفيصل الرفاعي[1]

[1]قسم الهندسة الميكانيكية، كلية الهندسة، جامعة الأزهر،، مدينة نصر، 11884، القاهرة، مصر

[2]قسم الهندسة الميكانيكية، كلية الهندسة، جامعة الزقازيق، الزقازيق، 44519، الشرقية، مصر

البريد الاليكتروني للباحث الرئيسي*: mohammadabdoel-rahman.18@azhar.edu.eg

الملخص

تعتبر غرفة البخار واحدة من أكثر الطرق فعالية لتبديد الحرارة في المكونات الإلكترونية. تبحث هذه الدراسة تجريبيا في الخصائص الحرارية لغرفة بخار جديدة بدون فتيل مدمجة مع بالوعة حرارية ذات زعانف مسطحة وذالك لتحديد ظروف التشغيل المثلى لغرفة البخار وتحسينها باستخدام سوائل مختلفة. تتناول الدراسة تأثير العوامل المختلفة مثل رقم رينولدز، مدخلات الحرارة، نسبة الملء، ضغط فراغ التشغيل، والسوائل المختلفة (الماء النقي ومحاليل البروبيلين جليكول) على الأداء الحراري لغرفة البخار. ولإثبات فعالية غرفة البخار، تم مقارنة الخصائص الحرارية للبلوعة الحرارية ذات الزعانف المسطحة مع وجود الغرفة وبدونها. توضح النتائج أن استخدام غرفة البخار يؤدي إلى توزيع درجة حرارة أكثر اتساقًا بشكل ملحوظ على

طول قاعدة بالوعة الحرارة ودرجات حرارة إجمالية منخفضـــة. على العكس من ذلك، في حالة عدم وجود غرفة البخار، يُظهر توزيعًا غير منتظم لدرجة الحرارة، مع شكل جانبي على شكل جرس ودرجات حرارة عالية مركزة في المركز في نفس ظروف التشـغيل. بناءً على النتائج التجريبية، فإن أقل مقاومة حرارية على مدى مدخلات الحرارة (10 – 90 واط)، وأقل درجة حرارة للسخان تحدث عند نسبة ملء 50% مع ضغط فراغ التشغيل = 1 كيلو باسكال. يتحسن الأداء الحراري لغرفة البخار باستخدام محلول البروبيلين جليكول عند مدخلات حرارة منخفضة.

الكلمات المفتاحية: غرفة البخار، الأداء الحراري، بالوعة الحرارة و المقاومة الحرارية.

1. INTRODUCTION

The thermal control of electronic devices has received significant attention in research and development over the past few decades due to the continued advancement of electronic devices. Electronic devices create a highly concentrated heat flux, known as a hotspot, which could cause the complete electronic device to malfunction [1-3]. Therefore, the thermal spreading or thermal distribution of hotspots in electronic devices is a common problem. Conventional cooling methods such as increasing the area of heat sinks or using forced convective air cooling by the fan were extensively used in electronic cooling technology, but these methods have limitations. One of the primary challenges with these methods is that they often do not distribute the heat uniformly, which can lead to hot spots and local overheating.

Vapor chambers (VC) are commonly used to cool electronic devices [4, 5]. A VC is a highly effective and efficient heat spreader used in electronic devices [6-8] such as hard disk drivers [9], smartphones [10], LEDs [11-13], photovoltaic [14], solar collectors [15], and fuel cells [16–18]. A vapor chamber (VC) is a flat vacuum vessel made of copper or other materials. The VC contains a small quantity of liquid such as water or other liquid coolants. The vessel sides may be lined with or without wick structures [19]. The generated heat by an electronic component such as a CPU in a laptop is transferred to the VC by conduction through thermal grease (commonly used as an interface material between heat sinks and the CPU) [20]. This heat causes the liquid inside the evaporator section to vaporize, creating a vapor that flows to the cooler condenser section. The vapor loses the heat at the condenser section and condenses back into liquid form. The condensed liquid then returns to the evaporator section by either capillary effect or gravity, creating a continuous cycle that effectively cools the electronic device. There are many working studies to investigate the VC's thermal performance.

The thermal performance of an aluminum VC heat sink is investigated experimentally [21], which used acetone as a working fluid and micro stainless steel wick structures fabricated by the metal etch. The results found that a filling ratio of 30% yielded the best thermal performance. While a copper VC without a wick which used distilled water as a working fluid is investigated experimentally [22]. The results show that the VCs are a better way to spread heat than traditional solid metal heat sinks under the same conditions.

The experimental comparison of using magnetic working fluid and water in a copper disk-shaped VC without a wick structure is studied [23]. The results found that magnetic fluid may be a promising alternative to traditional working fluids for VC, and the optimum charge ratio for the magnetic fluid was 53.5%. The thermal performance of a copper annular-shaped VC without a wick structure using different working fluids is investigated experimentally [24]. The study found that the VC's thermal performance using water as a working fluid was much better than that using methyl alcohol. The study also indicated that the optimum charge was 30% for most tested working fluids.

The heat transfer of an aluminum VC without a wick structure is investigated experimentally [25]. The study found that increasing the operating vacuum pressure improved thermal performance. Additionally, using acetone as the working fluid resulted in a thermal performance better compared to water. The heat transfer characteristics of a wickless VC during condensation and evaporation are investigated experimentally[26]. The study found that the thermal behavior increased as the power input increased, and the 33% filling ratio is the optimum for overall heat transfer performance. The heat transfer characteristics of a heat sink with VC are investigated numerically [27]. In a VC utilizing acetone as the working fluid, the study shows that the thermal resistance of the integrated heat sink vapor chamber (IHSVC) decreased by 49.6% as the heater area increased by a factor of 1.25.

This review shows that the vapor chamber (VC) is one of the most effective methods for heat dissipation in electronic devices and the challenge to dissipate the generated heat from electronic devices properly and uniformly and overcome hotspots (local overheating) is an open topic despite valuable research efforts. This work investigates experimentally the thermal performance enhancement of a PFHS integrated with a new design of a wickless vapor chamber across a range of operating conditions. The effects of parameters including Reynolds number, heat input, vacuum pressure, fill ratio, and different working fluids are analyzed. This research contributes to the enhancement of heat dissipation in electronic devices, addressing the growing demand for efficient thermal control.

2. EXPERIMENTAL SETUP

The experimental setup and measuring tools are illustrated in Figure 1. The setup consisted of a wind tunnel as its primary component, the wind tunnel is divided into three main parts: the bell mouth, the test section, and the centrifugal fan. The air is drawn into the wind tunnel by a centrifugal fan powered by a 1 hp electric motor. The bell mouth is used to create a uniform flow of air as it enters the wind tunnel. A thermocouple was placed at the inlet of the wind tunnel to measure the air inlet temperature.

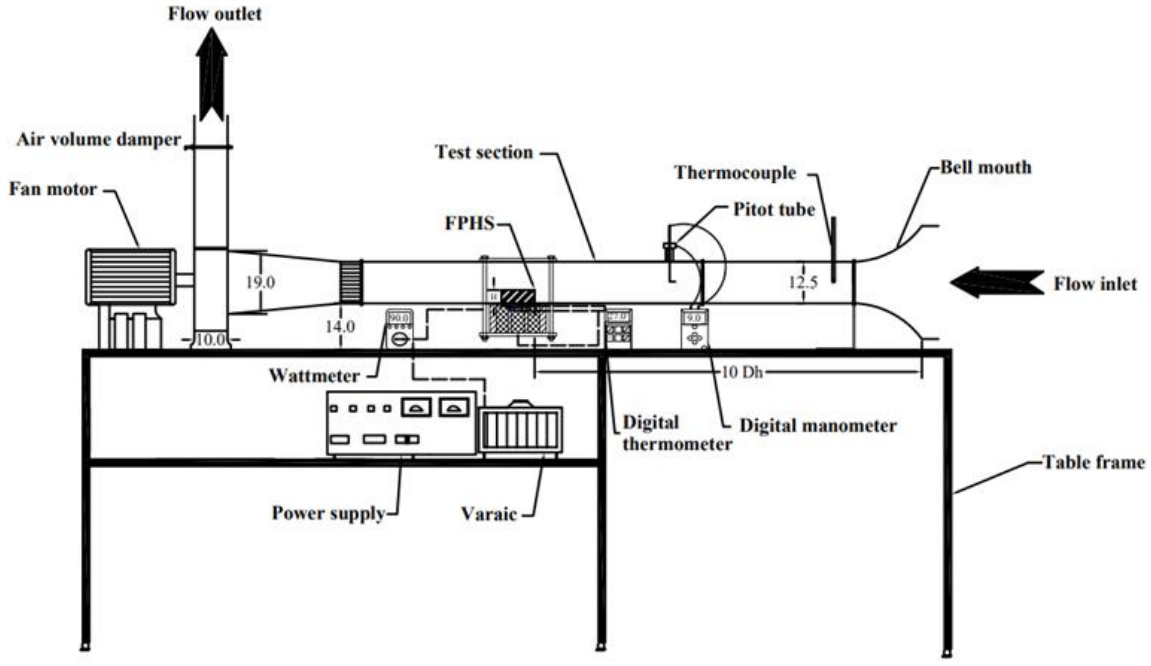

Fig. 1: Setup components and measuring tools.

2.1. Test Section

A test section consists of a main duct made from a 6 mm thickness Plexiglas plate and assembled tightly to prevent air leakage. The main duct has a square cross-section with 125 mm sides and a 1000 mm length. PFHS integrated with VC is assembled with the main duct through a hole opening at the middle of the Plexiglas duct base in dimensions (100 mm x 100 mm). The PFHS was made from aluminum alloy 2017, with dimensions 100 mm*100 mm*40 mm, base thickness (t_b) = 5 mm, fins height (H) = 35 mm, fins thickness (t) = 1.5 mm, and with a fins number (N=16). To measure the temperature distribution of the PFHS base, five T-type thermocouples (copper-constantan) were placed on the PFHS base, as shown in Figure 2.

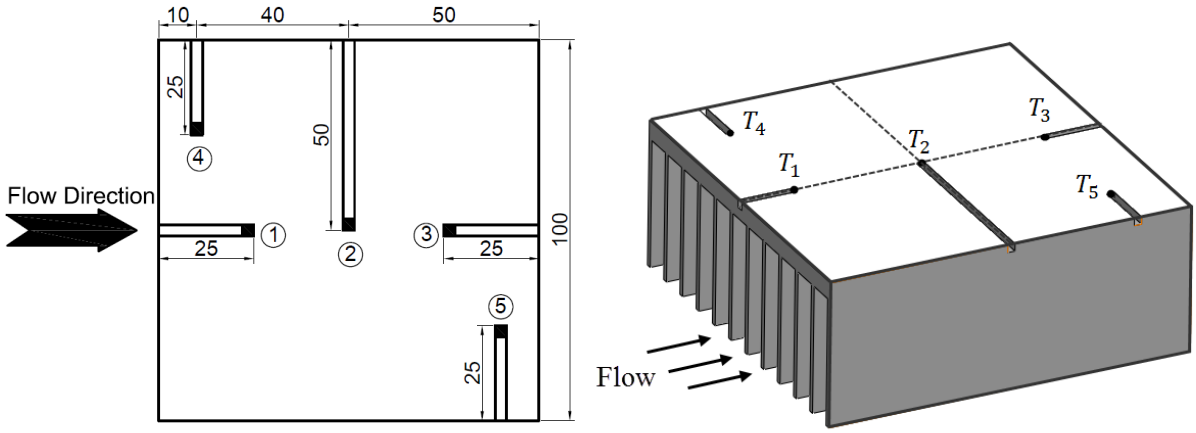

Fig. 2: PFHS configuration and thermocouples location.

(a) Plan view of PFHS. (b) 3-D of PFHS.

2.2. The Vapor Chamber (VC)

A wickless VC was constructed and designed as illustrated in Figure 3. The tested VC comprises two main parts: the chamber, and the top plate. The chamber and top plate were held together by circumferential bolts. To prevent leakage, a suitable O-ring was used. The five columns built in the chamber have the same chamber height (3.5mm height) to prevent deflection in the top plate during the vacuum. The VC is made from copper and has outer dimensions of 100 mm x 100 mm x 6 mm and inner dimensions of 80 mm x 80 mm x 3.5 mm. The charging valve was used to charge working fluid easily. To ensure the (VC) is sealed properly, a leakage test is performed. An air compressor pressurizes the VC to approximately 1.5 bar gauge pressure. The VC is then submerged in a water bath to check for any escaping air bubbles that would indicate a leak. Once no leaks are detected, the VC is prepared to charge with working fluid (distilled water).

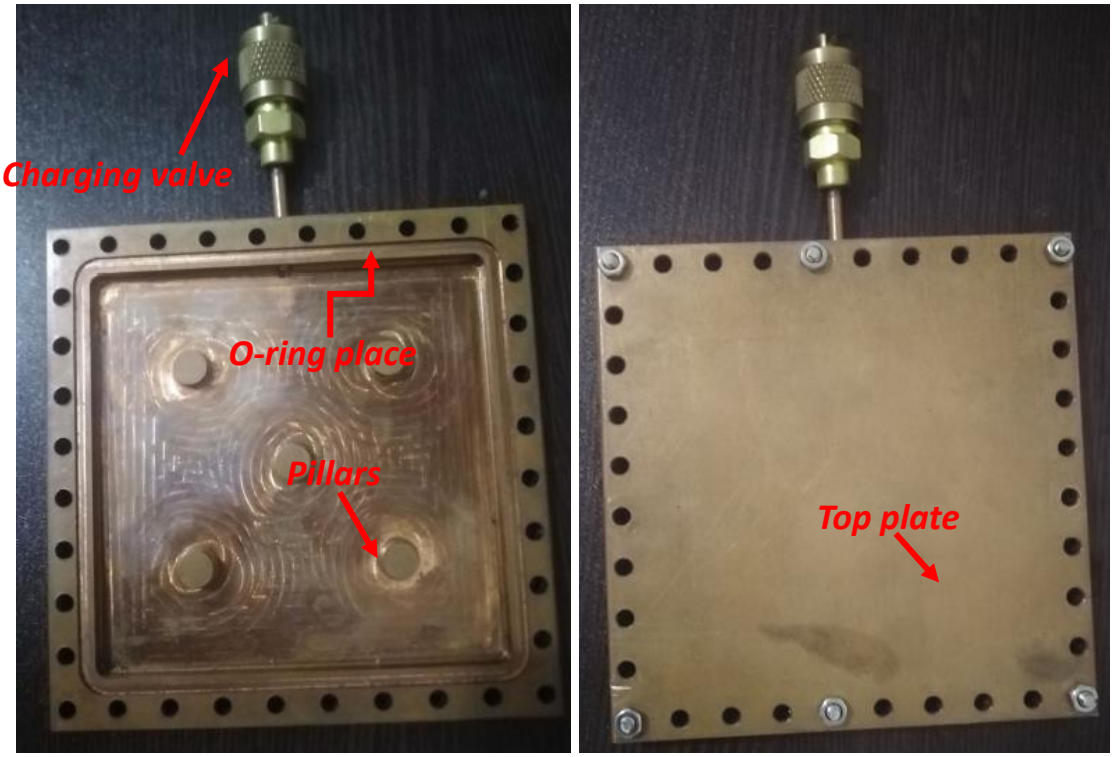

Fig. 3: Photos of the VC Configuration.

2.3. The Heat Source

The Heating source consists of a heater block and two electric pencil heater elements with 60 W each. The heater block is made from copper with dimensions of 30mm x 30mm x 5mm at the top and 50mm x 50mm x 10mm at the base of the heater. To maintain a constant heat flux, a variable AC power supply is utilized, and to control the electrical voltage, and current to the heater elements a varaic is utilized. The digital wattmeter is used to measure power (P_{input}) to the heater elements. The heating source is placed inside a wooden frame and insulated by glass wool, which has a thermal conductivity of (k = 0.023 W/m.K) to minimize heat losses. The assembly of the heater block and heater elements with the FPHS with VC is illustrated in Figure 4.

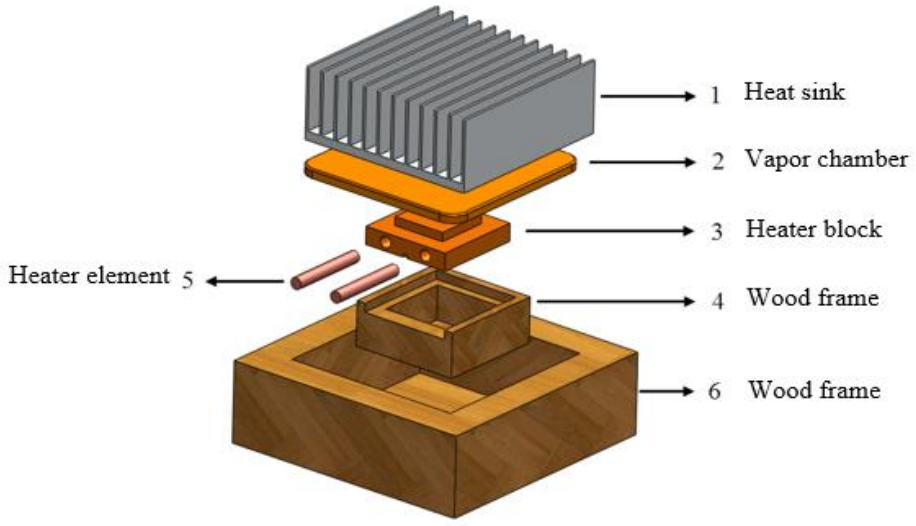

Fig. 4: The PFHS with VC and heating source assembly.

2.4. Charging Process

The charging unit consists of several components: a vacuum pump, valves, an injector (syringe), and a pressure gauge, as shown in Figure 5. To begin the suction process, follow these steps: close all valves initially, start the vacuum pump, then sequentially open valves numbered (1), (2), and (4) to create a vacuum within the VC until reaching the desired operating vacuum pressure. Afterward, close valves (4), (2), and (1) in the same order, and turn off the vacuum pump. Disconnect the VC from the suction unit to weigh the empty VC using a digital weighing scale with a readability of 0.01 g (Chyo-petit balance). Reconnect the VC to the charging unit to fill it with distilled water, adhering to the specified filling ratio. Open valves numbered (3) and (4) to allow the entry of distilled water into the VC, naturally by the pressure difference between the VC and the syringe. Re-weigh the VC to verify that the correct amount of distilled water has been charged. The preparation of the required quantity of distilled water involves the following steps: Begin by weighing the empty injector (syringe), then proceed to fill the syringe with the corresponding volume of distilled water according to the filling ratio. Subsequently, weigh the syringe containing the distilled water to determine its weight. Finally, charge the VC with the appropriate filling ratio and position it on the evaporator side of the heating source, while placing the heat sink on the condenser side. To further enhance heat transfer, apply a thin layer of thermal paste with a thermal conductivity of K = 1.9 W/m.K between the VC and the heat sink, as well as between the VC and the heater.

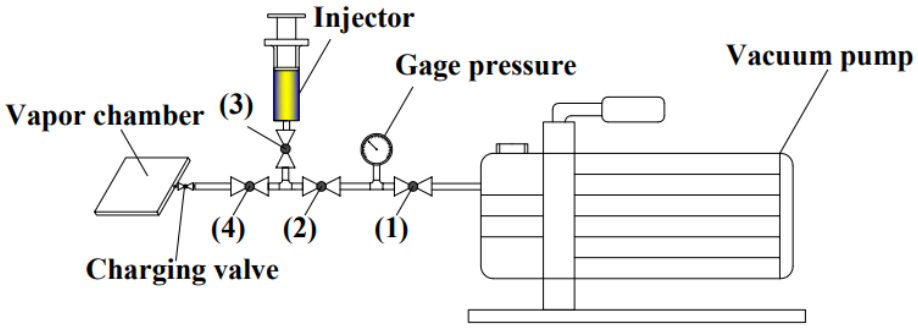

Fig. 5: Schematic of the charging unit components.

3. EXPERIMENTAL PROCEDURE

Initially, distilled water is used as a working fluid, and investigated the the thermal characteristics of VC under different conditions to obtain the optimum operating conditions, Then several concentrations of propylene glycol water solutions are used as a working fluid to investigate VC thermal performance under the optimum operating conditions obtained. Table 1 shows the range of different factors in which a series of tests were carried out.

Table 1. The range of parameters in the study

Parameter	*Value*	Unit
heat input range(Q)	10 - 90	W
Number of Fins (N)	8 – 16	
Flow Re	15,580 - 62,310	
VC. filling ratio (FR)	10 - 70	%
VC. working fluid	Distilled water and Propylene glycol solution (10%, 20%, and 30%)	
VC. operating pressure	1 - 10	kPa

3.1. Experimental Procedure and Data Reduction.

The air velocities in the wind tunnel (U = 2, 4, 6, and 8 m/s) are determined by $U = \sqrt{\frac{2\Delta P}{\rho_a}}$ [m/s] where ΔP is pressure head [Pa], measured by a digital differential pressure manometer (Model: HD755, with range ±350 mm H_2o, and accuracy ±0.01% mm H_2o) using a pitot tube at entrance of test section and ρ_a is air density, [kg/m3]. The air velocity in the wind tunnel is controlled by a damper located at the wind tunnel outlet. The air inlet temperature (T_a) is measured by using a digital thermometer (Model: OMEGA: HH21A, with range 0: 400 ℃ of type T, and accuracy ±0.1% + 0.6 ºC) located at the wind tunnel inlet. The input electric power to the heater (P_{input}) is measured by a wattmeter device (Model: UT230B-EU, with range 0-3680 W, and accuracy ±1%) and adjusted via variac. The temperatures of the PFHS base (T_1, T_2, T_3, T_4, and T_5), heater temperature ($T_{h\,up}$), and insulation temperatures ($T_{ins\,up}$ and $T_{ins\,down}$) are measured at a steady state condition via a digital thermometer using thermocouples type T. As shown in Figure 6 the heat loss (Q_{loss}) from the heater to its surroundings via insulation may be computed using the following Equation (1):

$$Q_{loss} = K_{ins} A_{ins} \frac{T_{ins\,up} - T_{ins\,down}}{H_{ins}} \quad (1)$$

Where H_{ins} is insulation's height = 65mm and A_{ins} is the cross-section area of the insulation, therefore, the heat input can be obtained by Equation (2):

$$Q = P_{input} - Q_{loss} \quad (2)$$

The VC's thermal resistance R_{VC} can be calculated using the following Equation (3):

$$R_{VC} = \frac{T_{h-up} - T_{b_{av}}}{Q} \quad \text{where} \quad T_{b_{av}} = \frac{\sum_{i=1}^{i=5} T_i}{5} \quad (3)$$

The Nusselt numbers Nu_{Dh} of the heat sink can be estimated by Equation (4):

$$Nu_{Dh} = \frac{h\, D_h}{K_f} \quad (4)$$

Where D_h is the hydraulic diameter of the wind tunnel estimated by $D_h = {}^{4A}/_{P}$, K_f is the thermal conductive of the air taken at $T_{mean} = \frac{T_{bav}+T_a}{2}$ and h the heat transfer coefficient can be estimated by Equation (5):

$$h = \frac{Q}{A_{conv}(T_{bav} - T_a)} = \frac{1}{A\, R_{th}} \quad (5)$$

Where A_{conv} is the convective area of the heat sink.

Reynolds Number (Re) calculated by Equation (6):

$$Re = \frac{U_a . D_h . \rho_a}{\mu_a} \quad (6)$$

Where ρ_a is the air density, U_a is the airflow velocity (=2m/s: 8 m/s), and μ_a is given by Equation (7) [28]:

$$\mu_a = \mu_O \left(\frac{T_{a\,in}}{T_O}\right)^{0.7} \quad (7)$$

The filling ratio FR is obtained by Equation (8) [29]:

$$FR = \frac{V_{wf}}{V_{VC}} * 100 \quad \% \tag{8}$$

Where: V_{wf} is the working fluid volume, and V_{VC} is the inner volume of the vapor chamber. The Concentration of propylene glycol solution is obtained by Equation (9):

$$Concentration = \frac{V_{Propylene\ gylicol}}{V_{Total}} * 100\ \% \tag{9}$$

Where: V_{Total} is the total volume of solution (water +propylene glycol).

3.2. Uncertainty Analyses.

An uncertainty analysis was conducted to determine the total uncertainty in the derived parameter F by using the following Equation (10) [28].

$$\omega_F = \sqrt{\left(\frac{\partial F}{\partial x_1}\omega_1\right)^2 + \left(\frac{\partial F}{\partial x_2}\omega_2\right)^2 + \cdots\cdots\cdots\cdots + \left(\frac{\partial F}{\partial x_n}\omega_n\right)^2} \tag{10}$$

Where ω_F represents the uncertainty associated with the variable F, ω_1 denotes the uncertainty of parameter x_1, and $\frac{\partial F}{\partial x_1}$ is the partial derivative of F relating to x_1 .The measurement uncertainty and accuracy are determined by the uncertainty of the main measurements. The convective heat transfer coefficient of a heat sink is calculated based on measuring the heat load and temperatures. The T-type thermocouples are ±0.6ºC and the wattmeter has an accuracy of ±1 %. In Equation (10), substituted in the uncertainty formula, the uncertainty of the convective heat transfer coefficient accounted for ±1.03%d. Similarly, the thermal resistance and Nusselt number accounted for ±1.03 % uncertainty in the uncertainty analysis.

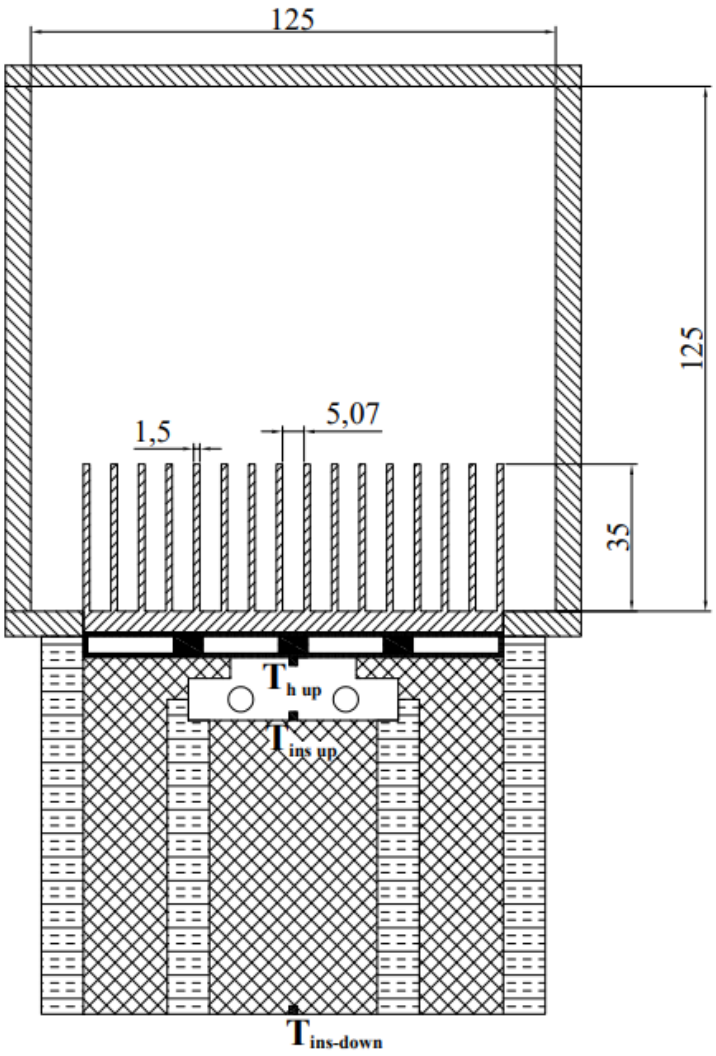

Fig. 6: A cross-section in a wind tunnel.

4. RESULTS AND DISCUSSION

4.1. Vapor Chamber With Distilled Water

4.1.1. Transient Behavior

The transient behavior of VC can be illustrated by the temperature difference between the upper heater temperature and air temperature due to the difficulty of stabilizing the ambient temperature during expermintal work. Figure 7 shows the transient behavior of VC utilizing distilled water as a working fluid at different heat inputs and constant Re=31,160. It is indicated that the time consumed to reach steady state conditions (i.e., the transient region) varied with heat inputs. For low heat input, a steady state is attained faster than for high heat input. The transient time for almost all heat inputs was approximately 1000 seconds.

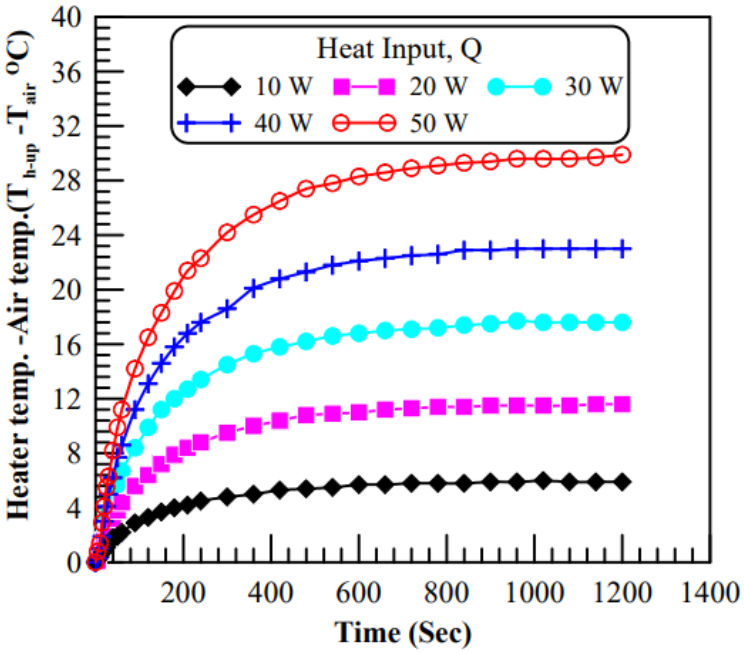

Fig. 7: Transient response of VC using distilled water.

4.1.2. Effect of Heat Input (Q)

Figure 8 depicts the influence of heat input on the thermal behavior of VC at various filling ratios and constant Re = 31,160. For all ranges of filling ratio, the VC's thermal resistance ($R_{\text{th VC}}$) decreases as heat input increases and vice versa. This could be due that at low heat inputs, the heat is enough to boil or evaporate the distilled water, therefore the heat is transferred from the heater to the heat sink by conduction mode. With increasing heat input, the temperature of the heater increases as shown in Figure 9, and the evaporation or the boiling of working fluid starts, and the thermal resistance reduces.

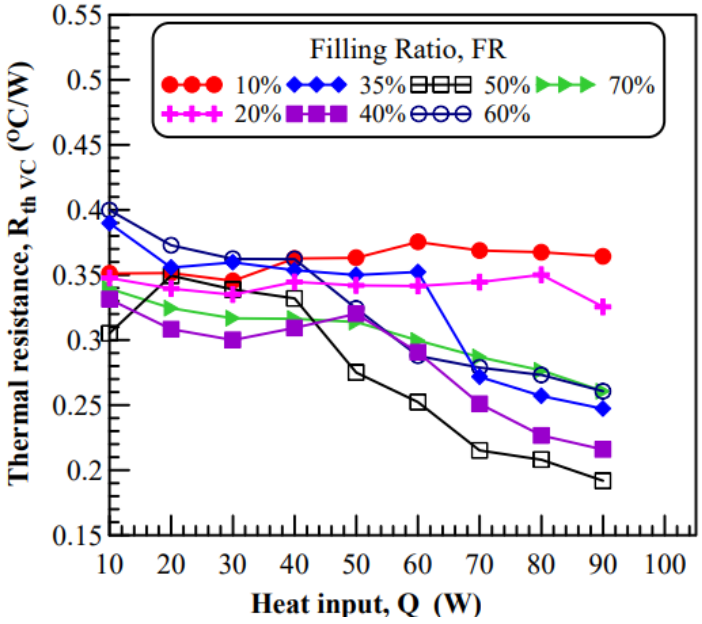

Fig. 8: The heat input effect on the VC's thermal resistance at various filling ratios (F. R).

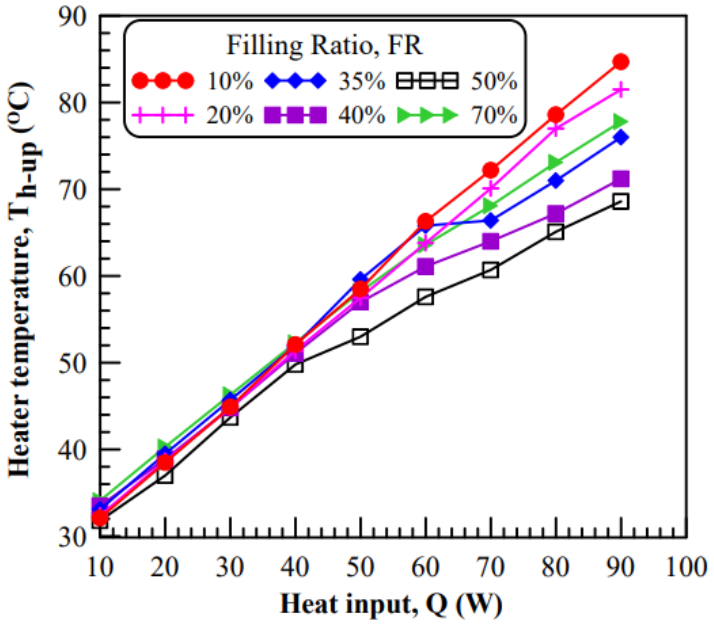

Fig. 9: The heat input affects heater temperature at various filling ratios (F. R).

4.1.3. Effect of Filling Ratio (FR)

The effect of the filling ratio (FR) on the VC's thermal performance at Re =31,160 and different heat inputs is shown in Figure 10. The VC's thermal resistance ($R_{\text{th VC}}$) decreases sharply as the filling ratio increases up to FR =50%. For the FR greater than 50%, the $R_{\text{th VC}}$ increases as the filling ratio increases as shown in Figure 10 (a). The effect of FR on the temperature of the heater (T_{h-up}) has the same trend. As shown in Figure 10 (b) the T_{h-up} increases as the filling ratio increases up to FR= 50%. For FR greater than 50%, the T_{h-up}increases as the filling ratio increases.

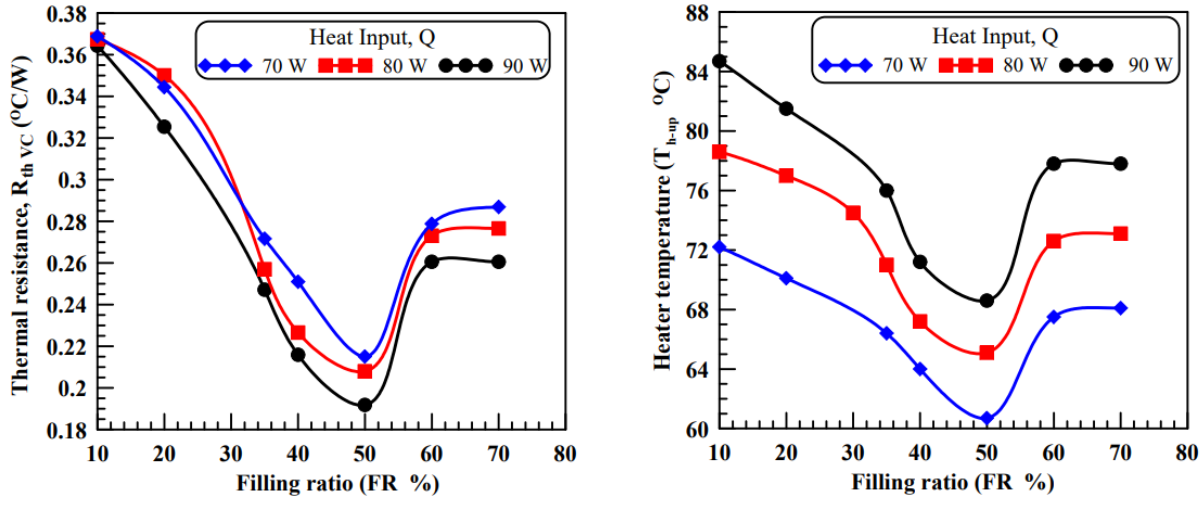

(a) (b)

Fig. 10. Effect of the filling ratio on the VC's thermal performance : (a) VC's thermal resistance ($R_{\text{th VC}}$) (b) Heater temperature (T_{h-up}).

4.1.4. Effect of the Operating Vacuum Pressure

The impact of the operating vacuum pressures on the temperature of the heater at FR = 50%, Re = 31,160, and different heat inputs are shown in Figure 11. The results indicate that the heater temperature with operating vacuum pressure =1 kPa is lower than the heater temperature at

other operating vacuum pressures, this may be due to the amount of residual air (no condensable gas) in the chamber is decreased with high the vacuum, therefore, decreasing the condensation and the boiling resistance and improving the heat transfer rate.

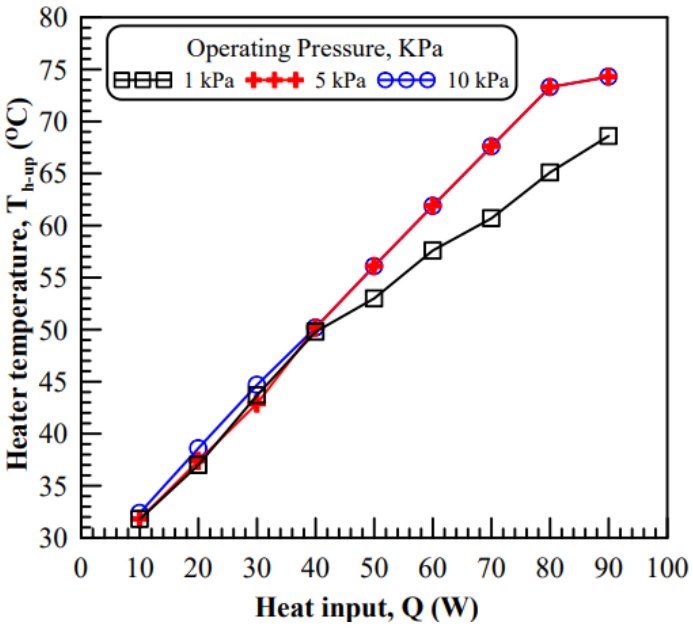

Fig. 11. The operating pressure affects the heater temperature.

4.1.5. Effect of Reynolds Number Re.

By analyzing the VC's thermal performance, it was discovered that its optimal operating conditions are a 50% filling ratio and a 90 W heat input. Thus, it was essential to investigate the Reynolds number (Re) effect on the VC's thermal performance under optimum operating conditions. This is depicted in Figure 12. The temperature of the heater decreases with an increase in the Reynolds number, and therefore the heat transfer rate via the VC will be faster, which will reduce the temperature of the heater, which is the desired goal of the study.

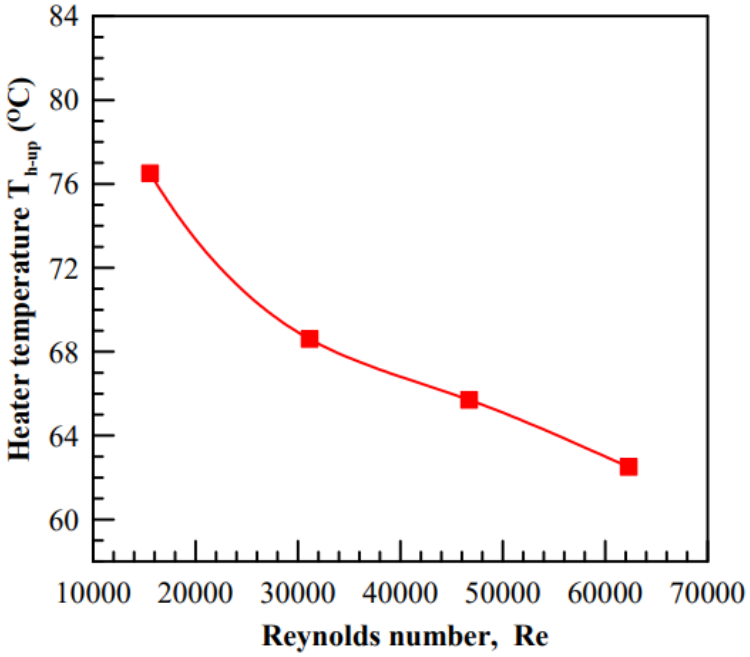

Fig. 12. Effect of Re on the heater temperature.

4.1.6. Temperature Distribution

Figure 13(a) shows the temperature distribution of the PFHS base with VC at various heat inputs. The temperature line maintains its form and the temperature difference between the center and edges remains below 3 ºC even with an increase in heat input up to 90 W. While Figure 13(b) shows a comparison of the temperature distribution of the PFHS base with VC and without VC Ref. [28] at fins number N = 16, heat input = 30 W, and Re =31,160. With the use of VC, uniform temperature distribution and reduced overall temperatures are obtained along the PFHS base. This is because thermal spreading resistance decreases due to a phase change occurring in the VC, heat can be removed rapidly, and a local high temperature is avoided. Without VC, non-uniform temperature distribution and the bell-shaped with local high temperature at the center are obtained along the PFHS base. Electronic devices can be damaged by local high temperatures. This means that the VC is more reliable for cooling electronic devices with high heat flux.

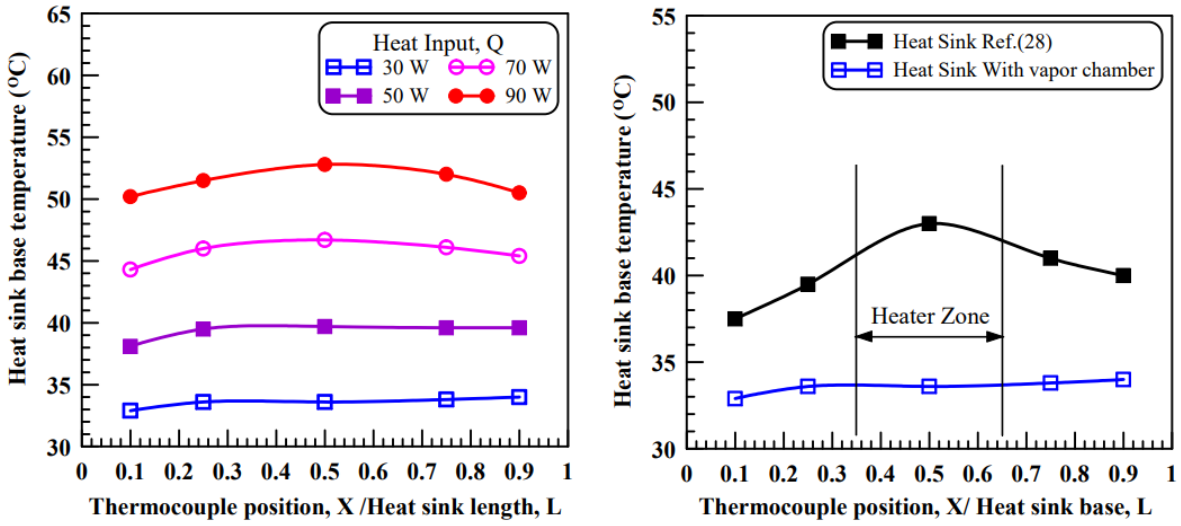

(a) (b)

Fig. 13: The temperature distribution of PFHS base: (a) With VC at different heat inputs (b) With and without VC at heat input, Q = 30 W

4.2. Vapor Chamber with Water Propylene Glycol Solution

Based on previous findings, it has been determined that the vapor chamber operates optimally with a filling ratio of 50% and a vacuum operating pressure of 1kPa. Therefore, in this section, we will examine the thermal performance of the vapor chamber under the same operating conditions, but with the utilization of a water-propylene glycol solution at varying concentrations as the working fluid.

4.2.1. Transient Behavior

Figure 14 shows the transient behavior of VC with 20% propylene glycol water solution as a working fluid at different heat inputs and constant Re=31,160. It is indicated that the time consumed to reach steady state conditions (i.e., the transient region) varied with heat inputs. As heat input is low, reaches a steady state faster than high heat input. The transient time for almost all heat inputs does not exceed 600 seconds. This is illustrated that with using Propylene glycol as a working fluid the steady state reaches faster than distilled water.

4.2.2. Effect of Heat Input (*Q*)

Figure 15 depicts the influence of heat input on the thermal behavior of VC's at several working fluids and constant Re = 31,160. For low heat input ,the VC thermal resistance with using propylene glycol water solutions as working fluids is lower than the VC's thermal resistance with using water, but for high heat input, the VC's thermal resistance with using water as working fluids is lower than the VC's thermal resistance with using propylene glycol water solutions. This is because the boiling temperatures of propylene glycol are higher than the boiling temperatures of water and when apply the heat, the water evaporates and separates from the solution. The amount of water in propylene glycol water solutions reduces as the concentration of propylene glycol increases, therefore when using a high concentration of propylene glycol the VC's thermal resistance increases at high heat input because it is needed large amount of water to evaporate and transfer the heat from evaporator to condenser. Thus, propylene glycol is recommended for low heat input but distilled water is recommended for high heat input.

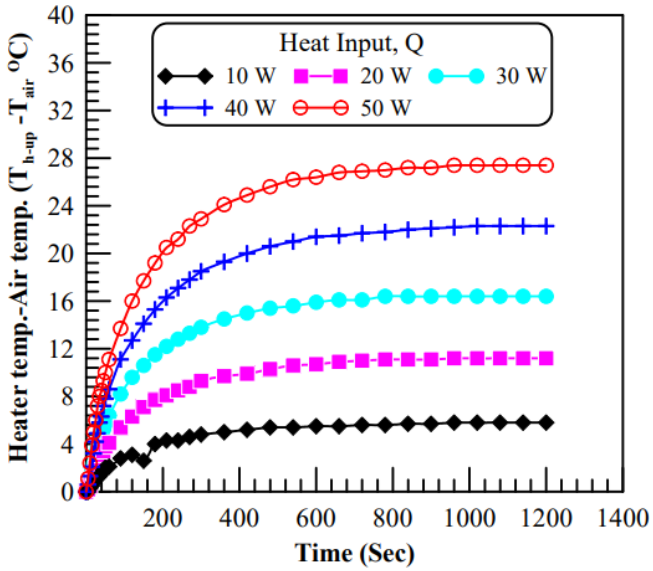

Fig. 14: Transient response of vapor chamber with using 20% propylene glycol water solution.

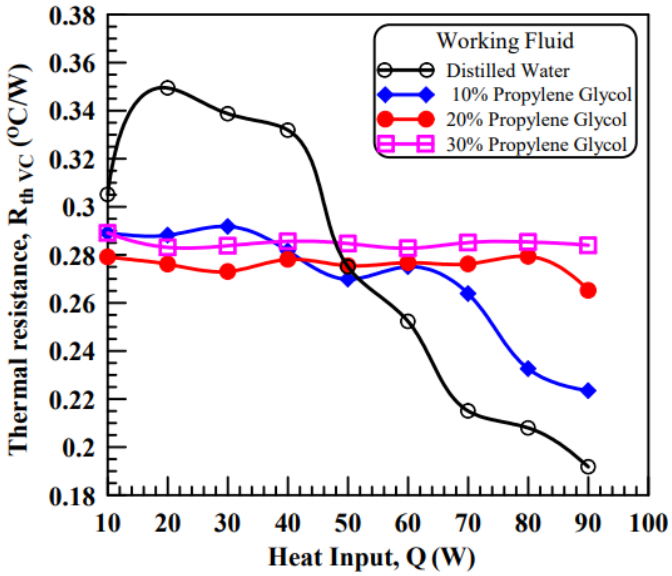

Fig. 15: Transient response of vapor chamber with using 20% propylene glycol water.

5. CONCLUSIONS

In this study, the VC's thermal performance was investigated experimentally. The effects of different factors such as heat input (Q), filling ratio (F. R), Reynolds number Re, operating pressure, and different working fluids were presented and discussed. The main results of this study are:
For distilled water as the working fluid:

1. As the heat input increases, the VC's thermal resistance decreases, thus the VC is more effective in high heat input.
2. The temperature of the PFHS base with a VC is more uniform compared with the temperature of the PFHS base without a VC. Therefore, a VC is more effective for spreading the concentrated heat flux.
3. For this VC, the optimum filling ratio is 50%, where the lowest heater temperature and the lowest thermal resistance are obtained at the filling ratio = 50% for all heat inputs.
4. The thermal resistance and heater temperature decrease as the operating vacuum pressure increases in the test pressure range. For this VC, 1 kPa seems to be the optimum working pressure.

For propylene glycol as the working fluid:

1. The VC reaches the steady state condition in a faster time not exceeding 600 seconds.
2. For low heat, propylene glycol is recommended as the working fluid, but for high heat input distilled water is recommended as the working fluid of VC.

ABBREVIATIONS:

A	The cross-sectional area[m2]	T	Temperature [oC]
D_h	Hydraulic diameter (m)	U	Velocity [m/s]
F.R	Filling Ratio [%]	V	Volume [m^3]
H	Height [m]		Subscript:
K	Thermal conductivity [W/m.K]	a	air
P	Perimeter [m]	avg.	average
P_{input}	Power input [W]	HS	heat sink
Q	Heat input [W]	Ins-up	insulation up
Re	Reynolds number	Ins-down	insulation down
R_{th}	Thermal resistance [oC/W]	VC	vapor chamber

REFERENCES

[1] Wu, G., Luo, Y., Bai, P., Wang, H., Cai, R., Tang, Y., Chen, X., Zhou, G., "Modeling and experimental analysis of an internally cooled vapor chamber", Energy Conversion and Management, 235, 2021, 114017.

[2] Liu, T., Yan, W., Yang, X., Wang, Sh., "Improving the thermal performance of thin vapor chamber by optimizing screen mesh wick structure", Thermal Science and Engineering Progress, 36, 2022, 101535.

[3] Bulut, M., Kandlikar, S. G., Sozbir, N., "A Review of Vapor Chambers", Heat Transfer Engineering, 40, 2019, 1551-1573.

[4] Hassan, H., Harmand, S., "A Three-Dimensional Study of Electronic Component Cooling Using a Flat Heat Pipe", Heat Transfer Engineering, 34, 2013, 596–607.

[5] Lia, B., Huang, K., Yan, Y., Lic, Y., Twahaa, S., Zhua, J., "Heat transfer enhancement of a modularised thermoelectric power generator for passenger vehicles", Applied Energy, 205, 2017, 868–879.

[6] Li Yi, Hu, H., Li, C., Zhang, Y., Yang, S., Pan, M., "Experimental investigation on enhanced flow and heat transfer performance of micro-jet impingement vapor chamber for high power electronics", International Journal of Thermal Sciences, 173, 2022, 107380.

[7] Wang, R.-T., Wang, J.-C., Chang, T.-L., "Experimental analysis for thermal performance of a vapor chamber applied to high-performance servers", Journal of Marine Science and Technology, 19, 2011, 353-360.

[8] Zeng, J., Zhang, S., Chen, G., Lin, L., Sun, Y., Chuai, L., Yuan, W., "Experimental investigation on thermal performance of aluminum vapor chamber using micro-grooved wick with reentrant cavity array", Applied Thermal Engineering, 130, 2018, 185–194.

[9] Naphon, P., Wongwises, S., Wiriyasart, S., "Application of two-phase vapor chamber technique for hard disk drive cooling of PCs", International Communications in Heat and Mass Transfer, 40, 2013, 32–35.

[10] Zhou, W., Li, Y., Chen, Z., Deng, L., Gan, Y., "Ultra-thin flattened heat pipe with a novel band-shape spiral woven mesh wick for cooling smartphones", International Journal of Heat and Mass Transfer, 146, 2020, 118792.

[11] Huang, H.-S., Chiang, Y.-C., Huang, C.-K., Chen, S.-L., "Experimental Investigation of Vapor Chamber Module Applied to High-Power Light-Emitting Diodes", Experimental Heat Transfer, 22, 2009, 26–38.

[12] Wang, J. C., "Thermal Investigations on LED vapor chamber-based plates", International Communications in Heat and Mass Transfer, 38, 2011, 1206 -1212.

[13] Lu, Z., Huang, P.F. B., Henzen, A., Coehoorn, R., Liao, H., Zhou, G.F., "Experimental investigation on the thermal performance of three-dimensional vapor chamber for LED automotive headlamps", Applied Thermal Engineering, 157, 2019, 113478.

[14] Jouhara, H., Milko, J., Danielewicz, J., Sayegh, M.A., Szulgowska- Zgrzywa, M., Ramos, J.B., Lester, S.P., "The performance of a novel flat heat pipe based thermal and PV/T (photovoltaic and thermal systems) solar collector that can be used as an energy-active building envelope material", Energy,108, 2016, 148–154.

[15] Wang, Z.-Y., Diao, Y.-H., Zhao, Y.-H., Wei, X.-Q., Chen, C. -Q., Wang, T.-y., Liang, L., "Compound parabolic concentrator solar air collection-storage system based on micro-heat pipe arrays", Solar Energy, 207, 2020, 743–758.

[16] Tetuko, A.P., Shabani, B., Andrews, J., "Thermal coupling of PEM fuel cell and metal hydride hydrogen storage using heat pipes", International Journal of Hydrogen Energy, 41, 2016, 4264–4277.

[17] Huang, B., Jian, Q.F., Luo, L.Z., Bai, X.Y., "Research on the in-plane temperature distribution in a PEMFC stack integrated with flat-plate heat pipe under different startup strategies and inclination angles", Applied Thermal Engineering, 179, 2020, 115741.

[18] Li, Y.Y., Chang, G.F., Xu, Y.M., Zhang, J.N., Zhao, W., "A Review of MHP Technology and Its Research Status in Cooling of Li-Ion Power Battery and PEMFC", Energy & Fuel 34, 2020, 13335–13349.

[19] Srimuang, W., Limkaisang, V., "A correlation to predict the heat flux on the air-side of a vapor chamber with overturn-U flattened tubes", Heat and Mass Transfer, 52, 2016, 1683–1692.

[20] Wiriyasart, S., Naphon, P., "Thermal performance enhancement of vapor chamber by coating

mini-channel heat sink with porous sintering media", International Journal of Heat and Mass Transfer, 126, 2018, 116–122.

[21] Go, J.S., "Quantitative thermal performance evaluation of a cost-effective vapor chamber heat sink containing a metal-etched micro wick structure for advanced microprocessor cooling", Sensor and Actuators A: Physical, 121, 2005, 549-556.

[22] Hsieh, S.S., Lee, R.Y., Shyu, J.C., Chen, S.W., "Thermal performance of flat vapor chamber heat spreader", Energy Conversion and Management, 49, 2008, 1774–1784.

[23] Ming, Z., Zhongliang, L., Guoyuan, M., Shuiyuan, C., "The experimental study on flat plate heat pipe of magnetic working fluid", Experimental Thermal and Fluid Science, 33, 2009, 1100–1105.

[24] Attia, A. A. A., El-Assal, B. T. A., "Experimental investigation of vapor chamber with different working fluids at different charge ratios", Ain Shams Engineering Journal, 3, 2012, 289–297.

[25] Peng, H., Li, J., Ling, X., "Study on heat transfer performance of an aluminum flat plate heat pipe with fins in vapor chamber", Energy Conversion and Management, 74, 2013, 44-50.

[26] Liu, Y., Han, X., Shen, C., Yao, F., Zhang, M., "Experimental Study on the Evaporation and Condensation Heat Transfer Characteristics of a Vapor Chamber", Energies, 12, 2019, 11.

[27] Ladekar, C., Pise, A., Nukulwar, M., Lingayat, A., "Comparative analysis of integrated heat sink vapor chamber with conventional heat sink for LED cooling", Materials Today: Proceedings, 72, 2023, 1136–1142.

[28] A. Al-Rahman, M.A, Ibrahim, S.A.A., Ahmed, S., Elrifai, M.E., "Thermo-hydraulic Characteristic Study of The Flat Plat-Finned Heat Sink", Journal of Al-Azhar University Engineering Sector, 69, 2023,951-972.

[29] A. Al-Rahman, M.A., Ibrahim, S.A.A., Elrifai, M.E., "Thermal Performance Study of Plate-Finned Vapor Chamber Heat Sink", Journal of Applied and Computational Mechanics. https://doi.org/10.22055/JACM.2023.44192.4177